

Short communication

Simulation of a thermal battery using Phoenixics[®]

Giancarlo C.S. Freitas^a, Fernando C. Peixoto^b, Ardson S. Vianna Jr.^{a,*}

^a Instituto Militar de Engenharia, Seção de Ensino de Engenharia Química, Praça General Tibúrcio, 80, Rio de Janeiro, Brazil¹

^b Universidade Federal Fluminense, Escola de Engenharia, Departamento de Engenharia Química e de Petróleo, Rua Passo da Pátria, 156 - Bloco D - Sala 307, 24210-240 Niterói, RJ, Brazil²

Received 19 October 2007; received in revised form 12 November 2007; accepted 13 November 2007

Available online 4 December 2007

Abstract

Thermal batteries are primary disposable systems specially designed to develop a high energy density in a short period. In the present work, the modeling of heat generation and propagation within three Ca/CaCrO₄ thermal batteries has been carried out, using a transient model. The commercial CFD software Phoenixics[®] has been used and, through a typical finite volume approach, the related 2D transport equations have been solved, giving the time-dependent temperature profiles. To check the quality of the model, the temperature of pseudo-equilibrium state (a typical thermodynamic parameter), has been analyzed. The temperatures related in the literature were close to those calculated. The results also indicate that the fusion of electrolytes is virtually an instantaneous process when compared to the time to reach the pseudo-equilibrium state, which indicates that the generation of electrical current occurs immediately after the thermite burning.

© 2008 Published by Elsevier B.V.

Keywords: Thermal batteries; Thermite; CFD; Modeling; Phoenixics[®]

1. Introduction

Thermal batteries are special electrochemical systems in which a great amount of energy is delivered during a relatively short period of time [1]. The cathode and the anode are juxtaposed to an electrolyte, which, at room temperature, is solid and inert. The start up is made by an electrical squibb that initiates a pyrotechnical material (thermite) placed between the cells. As can be seen in Fig. 1, the internal temperature rises quickly, melting the electrolyte and starting electrochemical reactions, which generates current densities much greater than those of typical batteries [2].

The advances in this technology were due to the employment of improved quality materials, cathodes and anodes in particular [2]. These improvements allowed the construction of more complex cells, which demanded laboratory tests to optimize their performance. The costs and time demands in assembling and

testing these more complex batteries are considerable high and computational simulations prior to experimental testing are of great assistance [3–6].

The main advantages of thermal batteries are: long shelf life time (up to 25 years), high reliability and improved resistance when exposed to dynamic charges, such as shock, vibration, acceleration and/or spin. These characteristics allow applications in defense devices and aerospace apparatus, such as missile guidance and control and additional energy supply for aerospace missions and satellites [7].

The thermal battery is an strategic technology mainly used in warfare systems, which causes a low availability of related scientific information in the open literature, most of the information being obtained from limited access technical reports, such as those held in Sandia Laboratory [8,9], QinetQ (formerly Defence Evaluation and Research Agency—DERA) [10] and Brazilian Army Technological Center [2]. As open references, we can mention the work of Nikitin et al. [11], which solves the heat balance equation in filter-press type batteries, Wu et al. [12], which studied the heat dissipation of lithium batteries, Butler et al. [13], which developed refinements useful to process multiple-cell and multi-tap testing and Schoeffert [14], which modeled the heat transfer within a Li/FeS₂ thermal

* Corresponding author. Tel.: +55 21 2546 7051; fax: +55 21 2546 7059.

E-mail addresses: gcantaluppi@gmail.com (G.C.S. Freitas), fpeixoto@vm.uff.br (F.C. Peixoto), ardson@ime.com.br (A.S. Vianna Jr.).

¹ www.ime.ub.br.

² www.uff.br/petroleo.

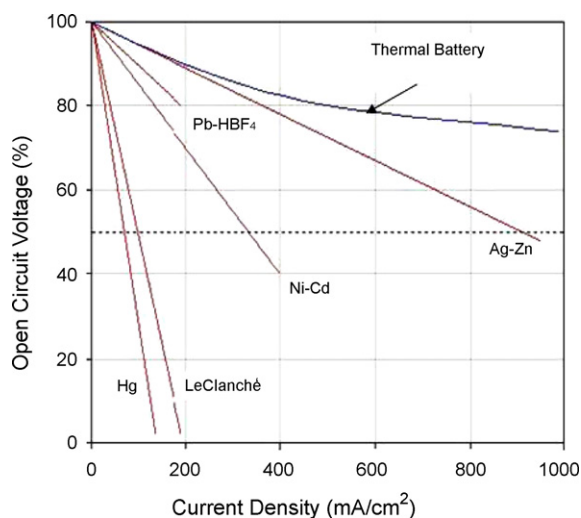


Fig. 1. Percentage of voltage in open circuit vs. current density (mA cm^{-2}).

battery and compared simulation results to experimental measurements.

In the present work, a transient model of heat generation and propagation within a Ca/CaCrO_4 (the so-called second generation) thermal battery is carried out, using a computational fluid dynamics (CFD) code. Briefly, CFD codes are computer programs devoted to solve the systems of equations governing heat, mass and momentum transfer. These systems are, typically, differential balance equations coupled with empirical rate equations (for example: Newton's, Fick's and Fourier's laws). The software, also, must use a suitable numerical method for the task (for example: finite element or finite volume methods) and provide an adequate graphical interface for both information input and output.

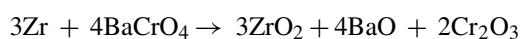
The simulations indicate that maximum electrolyte temperatures are similar to the temperatures mentioned in the literature as those produced by their open air burning. Besides, transient temperature profiles are similar to the results published by Schoeffert [14].

2. Fundamentals

The electrochemical system used in this work is the so-called second generation thermal battery, composed of a Ca/CaCrO_4 electrochemical scheme. It works at an average temperature of 600°C and its main elements are briefly described as follows.

Thermite is the heat source responsible for melting the thermal battery electrolyte, leading to device activation. It is a mixture of zirconium and barium chromate sustained by asbestos fibers in a circular shape [1,2].

The X-ray diffraction analyses of ashes resulting from Zr/BaCrO_4 thermite combustion in an argon atmosphere suggests a hypothetical decomposition reaction as formulated below [3]:



With this equation, thermal effects can be calculated, since the standard heat of reaction at 298 K (ΔH_{298}°) is [3]

$$\Delta H_{298}^\circ = -476.3 \text{ kcal mol}^{-1} \text{ of BaCrO}_4$$

The cathode is made by applying the electrochemically active material, CaCrO_4 and SiO_2 (also known as cathodic mixture) over a disc of pure nickel. To achieve this, a liquid matrix of trichloroethylene and dimethylphthalate is employed. The anode is made of pure metallic calcium and the electrolyte of the thermal battery is an eutectic mixture of inorganic salts applied on a glass fiber cloth for retention.

3. Methodology

3.1. Transient model construction

Three thermal battery designs are considered: 3-, 6- and 12-element cells. In a 3-element battery, for instance, there are seven thermite elements and nine electrolytes.

The transient model considered involves the ignition and the heat propagation until a pseudo-equilibrium temperature is achieved.

Each battery element was created in the software in its real dimension, respecting their true colors and using the materials in the software library. Thermites were defined as transient sources of energy with a thermal behavior that will be discussed later. Additionally, all thermites within the battery were assumed to be ignited at the same time and to burn at the same rate. The fact that all elements are pressed together was respected, leaving no void spaces between them. The space between the active elements and the outer case was "filled" with fiberfrax, defined as the domain material.

The natural choice of the coordinate system (R , θ and Z) was respected and the virtual domain had the dimension of the steel case, differing only in height, according to the type of battery in question (3, 6 or 12 unitary cells).

The heat transfer outside the battery is due to free convection and radiation. In a typical battery, in which diameter and height are both 3 in., a maximum of around 300 W of heat dissipation by (free) convection is expected. In the same way, the heat dissipation due to radiation is, coincidentally, around 300 W, assuming, in both cases, that the surface of the apparatus could achieve temperatures as high as 500°C . Since a single thermite generates around 12,000 J [3] of heat in approximately half second, the system can be considered adiabatic for our purposes. Additionally, additional thermites placed at the top and the bottom exactly compensate this heat loss [14].

In the real apparatus, the primary ignition is due to squibs attached to wall propagators made of thermite strips. Therefore, ignition of all the thermite happens almost at the same time. So, the initial simulation time was considered to be the one in which all the thermites are ignited; the dynamics of the propagators burning and their ignition by the squibs are outside the objectives of this work (besides, all these events happen in a very small period of time).

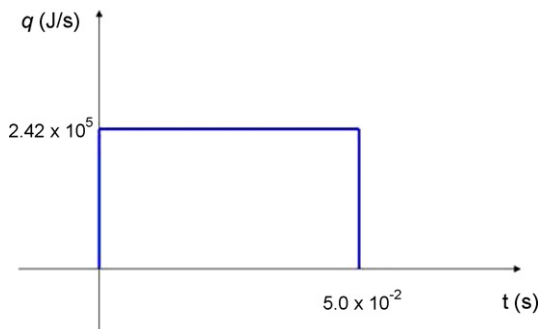


Fig. 2. Function pulse that performs mathematically the thermite burning.

High temperature variations are expected in the thermal battery, so the hypothesis of constant thermal conductivities and heat capacitances does not apply to the model developed here. As a result, mean values for those entities (for each substance) were calculated for an arbitrarily chosen temperature interval from 298 K to 902 K, assuming that this is the temperature range in the adiabatic system.

The burning velocity of Zr/BaCrO₄ mixture was assumed to be 0.56 m s⁻¹; attempts to accurately measure this parameter were tried, but until the end of this work, no conclusive results could be found. As there are two propagators in the battery and they act on two diametrically opposite points simultaneously, the burning time can be calculated as $t = \text{radius}/\text{burning rate} = 5.04 \times 10^{-2}$ s.

As already mentioned, previous works [3] employed a thermodynamic approach to calculate the heat produced by a single thermite, which was found to be 12,140 J.

The heat source of the thermal battery was modeled as a pulse function, which, on Phoenix[®], must be defined as shown in Fig. 2.

The final composition of each substance in cathode and anode was calculated and the temperature–average thermal conductivity and heat capacitance were obtained. In Phoenix[®] library, two new materials were created and labeled “cathode” and “anode” with their respective properties calculated as described.

3.2. Electrolyte modeling

The value for the KCl–LiCl eutectic mixture heat of fusion was the one mentioned in the comprehensive work of Masset and Guidotti [15]. Phase transition was modeled considering that the fusion occurs almost instantaneously (less than 0.5 s) and at a constant temperature. This assumption was made, because:

- the thinness of the electrolyte (0.10 mm) allows one to adopt the hypothesis that this element fuses completely—there is no need to establish a fusion mushy region in such a thin material;
- the fusion occurs at constant temperature, since the electrolyte is an eutectic;
- the heat propagation into the thermal battery occurs mainly by diffusion and convection can be neglected.

Additionally, it must be said that the void arising from the separator processing (electrolyte + binder) for the Li/FeS₂ reported in [16] is minimum in the present battery, and corresponding thermal effects were not be taken into account in the present system.

The remaining elements of the thermal battery had their properties estimated according to the material each of them was made of. This is the case of the activation base (made of bakelite), mica insulation sheets, separators (made of steel), negative pole (a nickel disk) and also fiberfrax that fills all the empty spaces after device mounting. All these elements could be found in the original library of Phoenix[®], besides fiberfrax, the properties of which were entered using the available supplier data-sheet.

4. Results and discussion

The results of the 3-element battery simulation will be discussed in greater detail only to show how the present methodology can be applied. Analogous analysis could be carried out for the 6- and 12-element batteries but we opted, for sake of simplicity, to merely mention the results for both.

The simulation of the 3-element battery showed that the pseudo-equilibrium temperature of the system (PET) is around 442 °C, but the optimum operation temperature (OOT) of this battery was found to be between 550 °C and 650 °C according to [2]. So, to ensure enough ionic mobility, the 3-element thermal battery could have its number of thermites increased for better efficiency. However, according to a more recent work [15], which mentioned the OOT to be between 350 °C and 550 °C, the present configuration would be already adequate.

In fact, as can be seen in these simulations – and could even be anticipated by the device anisotropy and by the existence of refractory materials in it – a situation of thermal equilibrium only can be achieved in a much longer time than that for the total consumption of the material with electrochemical activity. The OOT, however, was defined in the literature [2,15], so as to establish a parameter for calculation of the best amount of thermites. In this way, its comparison with the values of pseudo-equilibrium temperature (PET) obtained in this work will serve a qualitative and not a conclusive purpose for the acceptance of the experimental arrangement in question.

In Figs. 3–7 it can be observed the time evolution of temperature profiles for the 3-element battery, respectively at instants 4.44 s, 259.40 s, 745.50 s, 1121.00 s and 5505.00 s.

The simulation revealed that temperatures developed next to thermite locations, after its complete burning, is much greater than the equilibrium temperature, indicating that the elements next to the thermite (for instance, electrolytes) are subject to temperature peaks that can reach high values (up to 1000 °C). This fact is due to the high combustion heat of thermites, associated with its burning rate and by the final pressing operation of the device. Exhibiting only the objects of interest, Figs. 8–11 better illustrate that electrolytes heat quickly after the thermite ignition, allowing the time required for the eutectic KCl–LiCl fusion to be estimated.

Temperature profiles, similar to the ones depicted in Figs. 3–11, were found for the 6- and 12-element batteries but

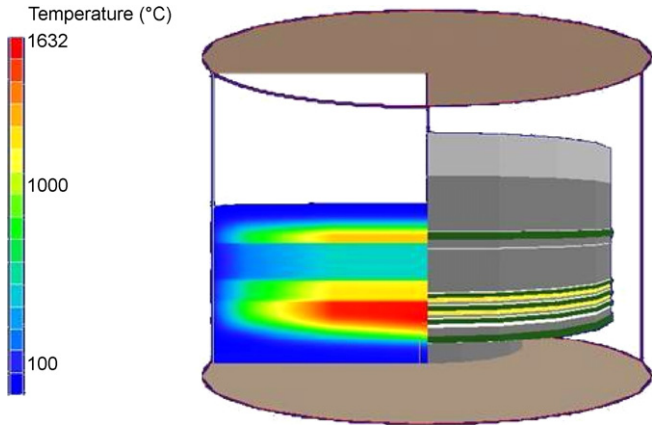


Fig. 3. Temperature profile in $t = 4.44$ s for the 3-element battery.

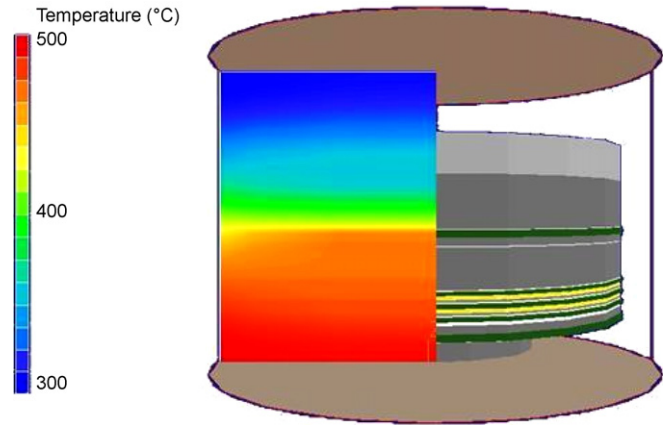


Fig. 6. Temperature profile in $t = 1121.00$ s for the 3-element battery.

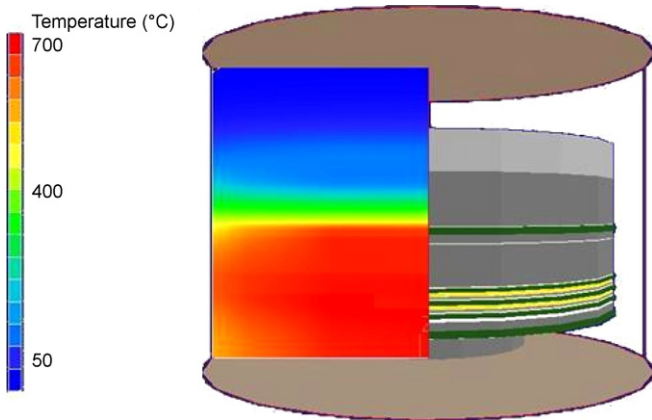


Fig. 4. Temperature profile in $t = 259.40$ s for the 3-element battery.

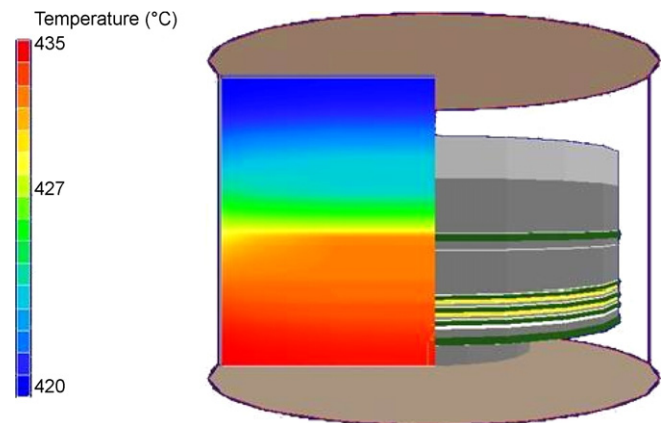


Fig. 7. Temperature profile in $t = 5505.00$ s for the 3-element battery.

the inclusion of the corresponding 18 figures were considered unnecessary, since they serve almost only for qualitative purposes.

It can be noticed that in $t = 1.2$ s, the electrolyte temperature exceeds the fusion temperature of eutectic (350°C). This shows that the activation of the battery is almost instantaneous, which is also observed in our laboratory tests.

The total computational processing time was around 6 h in an Athlon XP 1000 MHz with 256 Mb of RAM for each simulation

presented here. Results for all three configurations can be seen in Table 1.

From Table 1, it can be seen that the 3-element battery is the only one which presented a PET outside the acceptance range for OOT. This fact indicates that the number of thermites for such a device should be increased, in order to improve its electrochemical behavior.

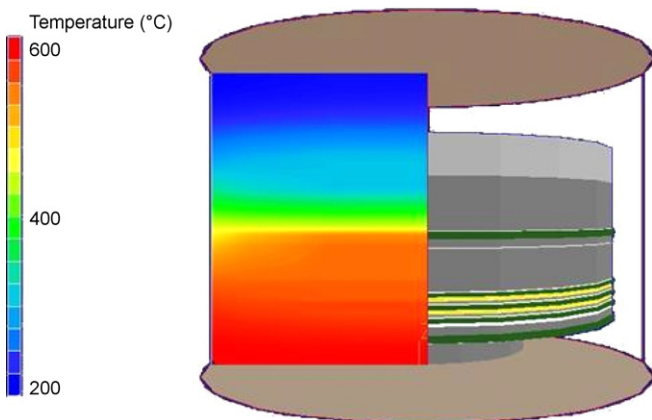


Fig. 5. Temperature profile in $t = 745.50$ s for the 3-element battery.

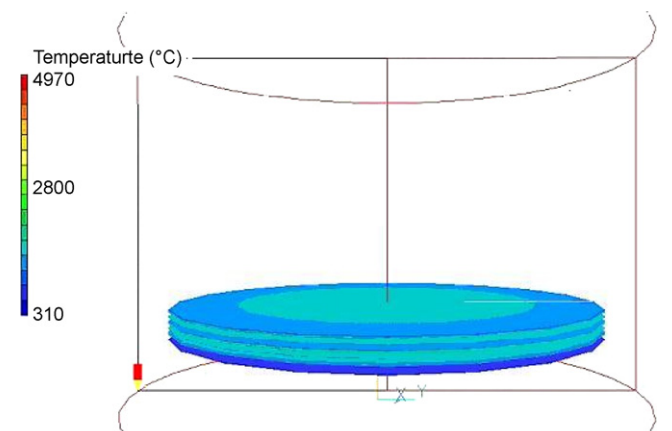


Fig. 8. Electrolyte temperature profile in $t = 0.48$ s for the 3-element battery.

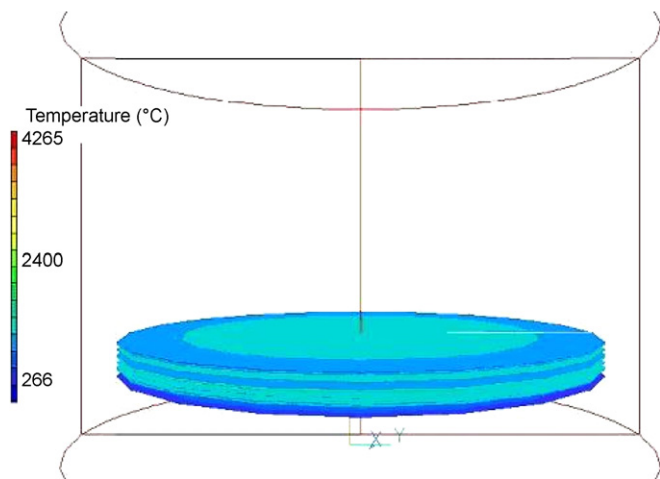


Fig. 9. Electrolyte temperature profile in $t = 0.80$ s for the 3-element battery.

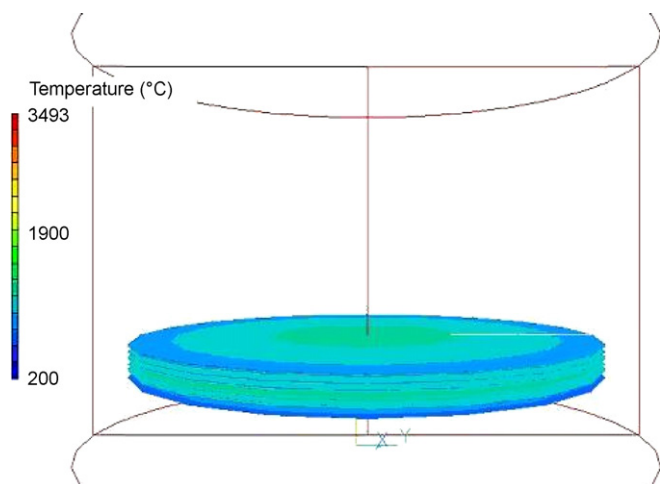


Fig. 10. Electrolyte temperature profile in $t = 1.20$ s for the 3-element battery.

To evaluate the effect of increasing the numbers of thermites for this device, two additional simulations were conducted, adding, respectively, one and two thermites, similar to those already present in the battery. The analysis times were the

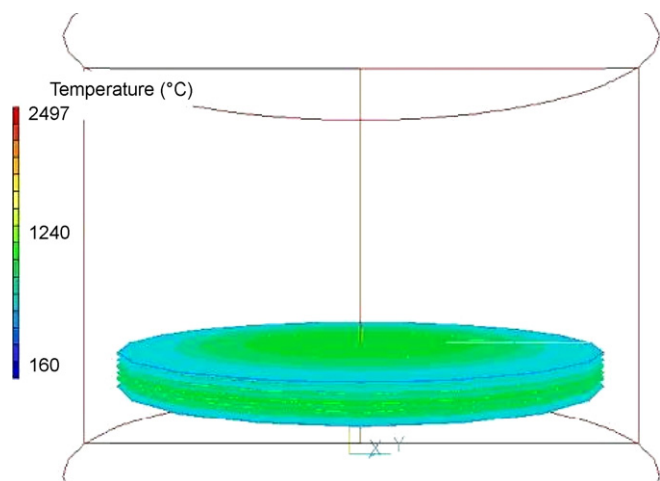


Fig. 11. Electrolyte temperature profile in $t = 2.00$ s for the 3-element battery.

Table 1
OOT \times PET

Number of elements	Calculated PET ($^{\circ}\text{C}$)	OOT ($^{\circ}\text{C}$)
3	440–442	550–650
6	550–555	550–650
12	643–684	550–650

Table 2

OOT vs. PET for the 3-element battery with supplementary thermites

Number of supplementary thermites	Calculated PET ($^{\circ}\text{C}$)	OOT ($^{\circ}\text{C}$)
0	440–442	550–650
1	500–505	550–650
2	550–556	550–650

same previously employed and the results are presented in Table 2.

The temperature versus time profiles for electrolytes, cathodes and anodes had shown no appreciable change, so the addition of one thermite may raise the working temperature – and, therefore, improve electrochemical behavior – without submitting electrolytes or electrodes to high temperatures, which could cause damage or undesired parallel reactions.

On adding two thermites, however, a change in the temperature profile of one electrolyte was noticed, which heated much faster. Nevertheless, the achieved PET in this case was 556°C , within the acceptance range, which indicates an improvement.

Therefore, simulations show that it is possible to improve 3-element battery behavior by adding one or two thermites, but the advantages and disadvantages of each case must be taken into account.

When adding only one supplementary thermite, a PET below the ideal range will be achieved, but the risk to the elements next to thermites is lower; whereas adding two thermites, one could raise the temperature to the ideal range mentioned in the literature, but at least one electrolyte will be subject to an undesired excessive heating, which could jeopardize the battery performance.

5. Conclusions

Despite thermal batteries having been invented in the 1940s, their improvement and optimization is still the subject of study and research. Since it is a device specially designed for defense applications, scientific articles are scarce, incomplete and do not reveal technical details for a complete technology description.

Concerning model construction, the results in this work indicate that the simplifications employed and the methodology adopted were adequate, because simulation results replicated those available in the literature, such as small battery action time—around 1.0 s or less. Also, the maximum electrolyte temperatures (those next to thermites) were similar to thermite adiabatic flame temperature (the one produced by open air burning) [3].

The pseudo-equilibrium temperature of Ca/CaCrO₄ batteries produced by the Brazilian Army Technological Center (CTEx)

and modeled in this work are within or quite close to the optimum operation temperature range related in the literature. It can be concluded that the dynamic simulation of such batteries are similar to the results published by Schoeffert [14] taking into consideration the particular characteristic of each system.

Acknowledgments

The authors gratefully acknowledge the reviewers' comments, some of which focused attention on interesting aspects that the authors had not notice at first.

References

- [1] R.A. Guidotti, Proceedings of the 27th International SAMPLE Technical Conference, 1995, pp. 807–817;
- R.A. Guidotti, P. Masset, *J. Power Sources* (2006) 1443–1449.
- [2] CTEX, Technical Report, Rio de Janeiro, 1999 (in Portuguese).
- [3] F.C. Peixoto, D.G. Santiago, A.A.M. Filho, M.T.C. Rupp, *Revista Matéria* [on-line: <http://www.materia.coppe.ufrj.br/mirror/sarra/artigos/artigo10061/index.html>], 2000 (in Portuguese).
- [4] J.D. Briscoe, C. Tobias, *Adv. Battery Syst. Div.* (1981) 686–691.
- [5] T. Yamauchi, K. Mizushima, Y. Satoh, S. Yamada, *J. Power Sources* 136 (2004) 99–107.
- [6] J. Newman, K.E. Thomas, H. Hafezi, D.R. Wheeler, *J. Power Sources* 119–121 (2003) 838–843.
- [7] B.V. Ratnakumar, M.C. Smart, A. Kindler, H. Frank, R. Ewell, S. Surampudi, *J. Power Sources* 119 (2003) 906–910.
- [8] D.M. Bush, R.L. Hughes, *A Thermal Model of a Thermal Battery*, Sandia Laboratories, 1979.
- [9] D.M. Bush, R.L. Hughes, *Computer Simulation of a Thermal Battery*, Sandia Laboratories, 1979.
- [10] J. Knight, I. McKirdy, *Proc. Int. Power Sources Symp.* 34 (1990) 141–144.
- [11] D.N. Nikitin, A.N. Yolshin, V.V. Zakharov, N.N. Batalov, I.V. Khmelevsky, *J. Power Sources* (1997) 285–286.
- [12] M.-S. Wu, K.H. Liu, Y.-Y. Wang, C.-C. Wan, *J. Power Sources* 109 (2002) 160–166.
- [13] P. Butler, C. Wagner, R. Guidotti, I. Francis, *J. Power Sources* 136 (2004) 240–245.
- [14] S. Schoeffert, *J. Power Sources* 42 (2005) 361–369.
- [15] P. Masset, R.A. Guidotti, *J. Power Sources* (2007) 397–414.
- [16] F.M. Delnick, R.A. Gudotti, *J. Electrochem. Soc.* (1990) 11–16.